Journal of Data Acquisition and Processing
ISSN: 1004-9037
https://sjcjycl.cn/
DOI: 10.5281/zenodo.7749979

TO STUDY ABOUT THE MANGANESE-BASED ELECTRODE MATERIALS WITH NANOARCHITECTURED FOR LITHIUM-ION BATTERY AND SUPER CAPACITOR APPLICATIONS

Mr.Serfraz Najeer Shaikh
Research Scholar, Electronics and Communication Engg. Dr.APJ Abdul Kalam University, Indore, India, serfrazshaikh@gmail.com

Dr.Rahul Mishra
Electronics and Communication Engg. Dr.APJ Abdul Kalam University, Indore, India rahulmishra@aku.ac.in

ABSTRACT

Li-ion batteries are secondary batteries with a Lithium anode and Li+ ions dissolved in carbon. The cathode material is composed of chemicals that liberate lithium. With a high energy density and low self-discharge, they are one of the most widely used rechargeable battery types for portable electronics. The lithium-ion battery has three times more energy than lead-acid or NiCd batteries of the same size and weight, and twice as much energy as NiMH batteries. For the same amount of energy, it is half the size and weight of a NiMH battery. These qualities have made lithium-ion batteries a key component in the advancement of the technological revolution. It has enabled the development of mobile phones with a wide range of features and powerful portable PCs. Li-ion batteries can also operate well in a wide temperature range, from -20 degrees Celsius to +50 degrees Celsius, and they can withstand hundreds of cycles of charging and discharging. It shouldn't be shocking that more research and development is being done on the lithium-ion system than any other system, or that the use of lithium-ion batteries is growing more quickly than the use of any other portable source of energy. Since the development of electrotechnology, electrostatic capacitors have been a crucial component of electronic circuits since they are the simplest and most literal method to store electrical energy. Supercapacitors have been used to complement or replace batteries in applications requiring energy storage and/or load-leveling, such as portable electronic devices, plug-in hybrid electric cars, wind farms, and long-term continuous circuits. Wind farms are one example of these kinds of uses. Due to their high cost and low energy density, supercapacitors have less market penetration when compared to batteries. Supercapacitors have a high power density, however this is the case. In essence, a supercapacitor is an electrochemical capacitor with a very high energy density. It typically comprises of two conductors (cathode and anode) that are separated by an insulator. Activated carbon-based conventional symmetric supercapacitors have intrinsically low energy density. Producing an asymmetric supercapacitor with a carbon cathode and transition metal oxide anode could provide a solution. However, early attempts at developing such supercapacitors were constrained by kinetic considerations to extremely thin electrode sheets, resulting in a relatively poor energy density.

KEY WORDS: Li-ion batteries, energy density, supercapacitors, Lithium anode, chemical energy.

1. INTRODUCTION

An apparatus that transforms chemical energy into electrical energy is a battery. The electrodes of a battery are where the redox reaction occurs, and an external electric circuit is used to transport electrons from one electrode to the next. An electrical power source called a battery is made up of many cells that are connected to one another inside of a single container and arranged in a certain manner. Despite the fact that the phrase "battery" is used rather often, the cell is the electrochemical unit that is utilised to produce or store electrical energy. One must think of a battery as being made up of one or more of these cells connected in series, parallel, or both depending on the output voltage and capacity needed in order to understand the differences between a cell and a battery. One of the most prevalent sources of direct-current electrical energy, batteries are used in a number of products, including portable electric and electronic devices, lighting equipment, cars, boats, aeroplanes, and ships. They serve as a backup or additional energy source in certain circumstances, while being the only source of power in others.

The main power sources for the next generation of electric vehicles (EVs), hybrid electric vehicles (HEVs), and portable electric markets will be lithium-ion batteries (LIBs) and supercapacitors (SCs). As a direct result of this, much effort has been made to create different energy storage technologies, which have recently attracted the interest of academics. Examples include lithium ion batteries and supercapacitors. A kind of energy storage technology known as lithium-ion batteries has a big capacity and can hold up to 180 W h kg1 of energy at a time. However, since they only use the surface of the active material, supercapacitors, also known as electrochemical double-layer capacitors (EDLCs), have a very low energy storage capacity (less than 10 W h kg1) but a very large power supply capacity (more than 10 kW kg1) [5-8]. The cathode materials may have an impact on both the battery's performance and the supercapacitor's behaviour. LiMn2O4 and LiNi0.5Mn1.5O4 nanostructures are well recognised as the components of cathode materials for Li-ion batteries. These nanostructures may be found as porous nanorod materials, hollow microspheres, multi-shelled holes, porous microellipsoids, nanorods, or spheres. They can operate at a faster rate and have been designed to have a longer lifetime. In comparison to pure LiMn2O4, Ni-replaced LiNi0.5Mn1.5O4 has a better energy density in both Li-ion batteries and supercapacitors. When contrasting the two materials, this is the case.

Recently, materials made of mixed transition metal oxides have been employed as cathodes in the manufacture of energy storage systems including lithium-ion batteries and electrochemical supercapacitors. Because mixed transition metal oxides may have intricate redox reactions at several metal positions within a single crystal structure, this is the case. Manganese (LiMn2O4, LiNi0.5Mn1.5O4), phosphates (LiFePO4, LiCoPO4), and silicates (Li2MnSiO4, Li2FeSiO4) are a few examples of the electrode materials used in energy storage devices. LiNi0.5Mn1.5O4 was originally reported as a cathode material for 3 V Li-ion batteries by Amine et al., while Dahn et al. studied the plateau at 4.7 V. The energy density of LiNi0.5Mn1.5O4 is 20 and 30% more than that of LiCoO2 and LiFePO4 due to its high theoretical capacity of 147 mA h g1

and its high working voltage of 4.7 V, respectively. 4.7 V is also a high operating voltage for LiNi0.5Mn1.5O4. The 1D porous nanorods that make up the LiNi0.5Mn1.5O4 cathode material have a capacity retention rate of 91% when tested at a rate of 5 C and offer a short channel for the diffusion of Li-ions. Additionally, consistent hollow spheres of LiNi0.5Mn1.5O4 were created using nanobuilding blocks, and they retained 95% of their capacity at 0.5 C after 100 cycles. The spheres' dimensions were expressed in micrometres. Although porous nano and porous sub-micron size LNMO particles have the capability to store more specific capacitance and better retain capacity, they were not included in any of the publications since the focus of all the study was on LNMO particles in the micron size range. As a result, we provided a novel technique of synthesis for the creation of nanostructures, namely microcubes, in our report on the research. When used in Li-ion batteries and supercapacitors, these nanostructures showed enhanced specific capacity as well as capacity retention.

In this work, we used a basic precipitation procedure using sodium carbonate and sodium sulphate as the precipitating chemicals to produce porous LNMO microcubes. TGA, XRD, and FE-SEM examinations were conducted to assess the structural and morphological properties of the porous LNMO microcubes that were produced. For the first time, the most likely way of producing spinel structure is unveiled and thoroughly discussed, along with the use of porous LNMO microcubes in lithium-ion batteries and supercapacitors.

2. RESEARCH METHODOLOGY

2.1.Synthesis of porous LNMO microcubes

The porous LNMO microcubes were created using the precursor (Ni0.25Mn0.75)CO3 microcubes. A simple carbonate and sulphate precipitation procedure was used to create the (Ni0.25Mn0.75)CO3 microcubes precursor. An aqueous solution comprising nickel sulphate (Merck, NiSO4H2O, 99 percent) and manganese sulphate (Merck, MnSO4H2O, > 99 percent) was first prepared. Solution A, which contained the cations Ni2+ and Mn2+, was progressively mixed with solution B for three hours. This resulted in the precursor of (Ni0.25Mn0.75)CO3 microcubes, which precipitated as a light green colour. After centrifugation, the produced product was repeatedly rinsed in ethanol and water before being dried for twenty-four hours in a vacuum oven at a temperature of 100 degrees Celsius. The already-obtained (Ni0.25Mn0.75) CO3 microcubes precursor was combined with a stoichiometric amount of LiOH, and the combination was then calcined at 800 °C for ten hours. As a result, porous LiNi0.5Mn1.5O4 microcubes might develop. Porous LiNi0.5Mn1.5O4 microcubes are shown to be synthesised using the schematic design in figure 1. A vacuum desiccator was used to keep the created porous LNMO microcubes while structural and electrochemical characterizations were being

done on them.

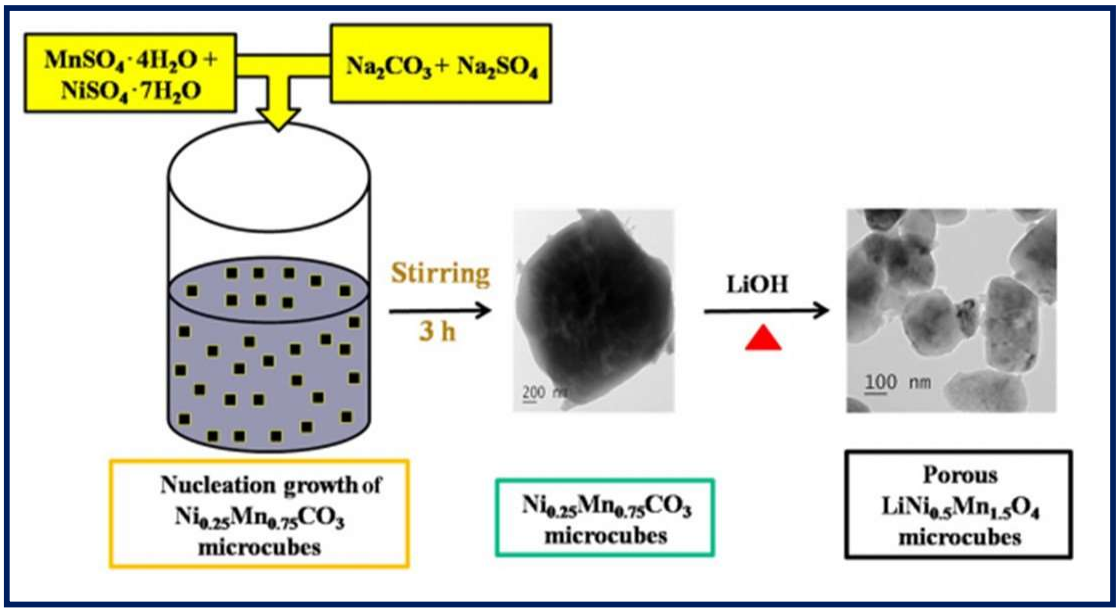

Figure. 1. A schematic diagram through precipitation method of porous LiNi0.5Mn1.5O4 microcubes

2.2.ELECTRODES PREPARATION FOR LI-ION BATTERY

Using a standard coin cell of the CR2032-type, the electrochemical capabilities of the created porous LNMO microcube cathodes in Li-ion cells were assessed. The working electrode in N-methyl-2-pyrrolidone is made up of 10% conductive carbon (Acetylene black, Sigma Aldrich, 99%), 80% active material (porous LNMO microcubes), and 80% polymer binder (polyvinylidene fluoride, Sigma Aldrich, 99%). (NMP, Fisher scientific 99 percent). On substrates constructed of aluminium foil, the active ingredients were coated, and they were then dried for ten hours at 120 degrees in an oven. The electrochemical cells were put together inside of a glove box, in a very dry and highly clean environment of argon. The cathode, a polypropylene (PP) separator, and a lithium foil anode make up the whole coin cell. To ensure the reliability of the cells designed for usage in high voltage applications, ethylene carbonate (EC) and dimethyl carbonate (DMC) were combined in a 1:1 volume/volume ratio with a 1.0 M LiPF6 electrolyte.

2.3. ELECTRODES PREPARATION FOR SUPERCAPACITOR

First, double-distilled water was used to clean the nickel foam that acted as the electrode substrate. Next, acetone was used to rinse the foam, and finally it was allowed to air dry. A coating of an active material slurry (consisting of 75% LiNi0.5Mn1.5O4, 20% Super P, and 5% PVDF suspended in a few drops of NMP) was applied on cleaned, one centimetre squared Ni-foam before it was baked at 100 degrees Celsius for 12 hours in a vacuum. A three-electrode setup was employed to conduct the electrochemical investigation. The created electrode (LNMO microcubes) acted as the working electrode while the saturated calomel electrode served as the reference electrode. On a CHI 6131D electrochemical analyzer, the

electrochemical properties of spinel porous LNMO microcubes employed in supercapacitor applications were examined using cyclic voltammetry (CV), charge-discharge, cycle stability, and electrochemical impedance spectroscopy (EIS) methods. These methods were utilised to examine the microcubes' electrochemical characteristics. The potential ranged between -0.6 and 0.45 V, and the CV measurements were performed using a variety of scan rates, ranging from 5 to 50 mV per second. Additionally, several current densities within the potential range of -0.6 to 0.4 V were used in the charge-discharge tests (0.75–2.5 A g1).

3. RESULTS AND DISCUSSION

3.1.TGA analysis

The synthesised combination of (Ni0.25Mn0.75)CO3 and LiOH was put through a thermogravimetric analysis (TGA), and the spectrum that was obtained is shown in Figure. 6.2. At varying temperatures, weight loss occurred in three stages: from 28 to 210 degrees Celsius, 210 to 350 degrees Celsius, and 350 to 652 degrees Celsius. Because of their hygroscopic nature and the fact that they have water chemically bonded to them, LNMO microcubes experience a superficial water loss that translates to a 24 percent weight loss in the initial weight loss that occurs between 28 and 210 degrees Celsius. The full removal of carbonate from the synthesis process (the –CO3 group) is the cause of the second weight loss of about 25 percent that is seen between 210 and 350 degrees Celsius. The third weight loss region occurs at temperatures between 350 and 652 degrees Celsius and is caused by the transformation of Mn3O4 into MnO2. In conclusion, there was not a discernible change in weight across the temperature range of 652–1000 °C. This indicates that the acquired sample of LNMO is stable at higher temperatures; hence, its calcination temperature was fixed at 800 °C for the synthesis of spinel porous LNMO microcubes.

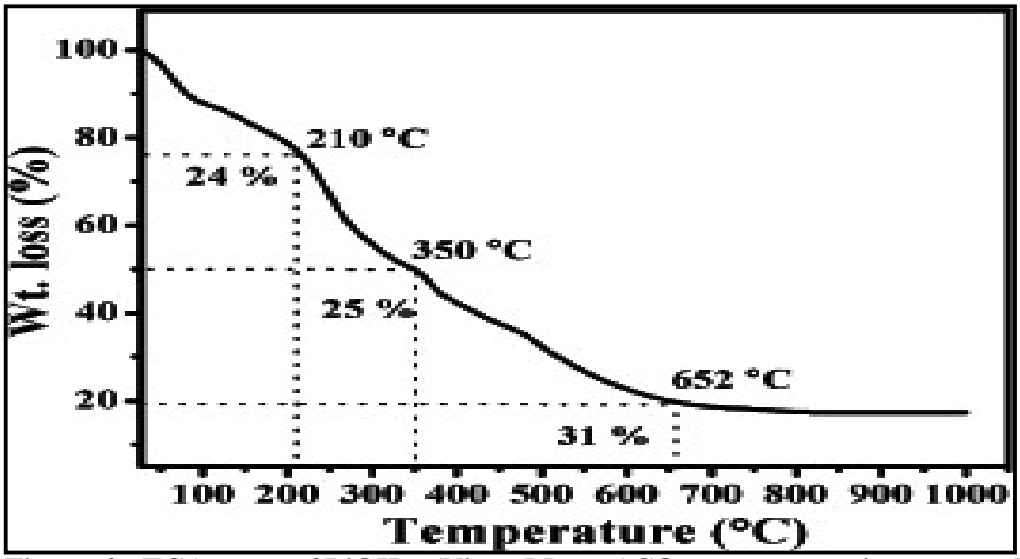

Figure. 2 TGA curve of LiOH + (Ni0.25Mn0.75)CO3 precursor mixture sample

3.2. XRD ANALYSIS

Figures 3a and 3b, respectively, depict the powder X-ray diffraction patterns of the produced precursor (Ni0.25Mn0.75)CO3 and the porous LiNi0.5Mn1.5O4 microcubes. The hexagonal structure of (Ni0.25Mn0.75)CO3, which has a space group of R-3c, is seen in Figure 3a. The spinel structure of LiNi0.5Mn1.5O4 with a Fd-3m space group is seen in Figure 3b . All of the (Ni0.25Mn0.75)CO3 diffraction peaks may be indexed to one of these two configurations (JCPDS Card No. 80-2162). The porous LNMO microcubes exhibited a highly crystalline structure, as seen by the diffraction peaks that were more clear and had a higher intensity. However, the development of the secondary phase of LixNi1xO or NiO, the byproducts of which are often seen to increase as the Mn/Ni ratio increases, may be connected to the emergence of the asterisk peaks at 37.6 degrees. Li ions were lost from the porous LNMO microcubes as a result of the high-temperature calcinations' reduction in the concentration of Mn ions. The synthesised porous LNMO microcubes have an average crystallite size of 54.9 nm, according to the Scherrer equation.

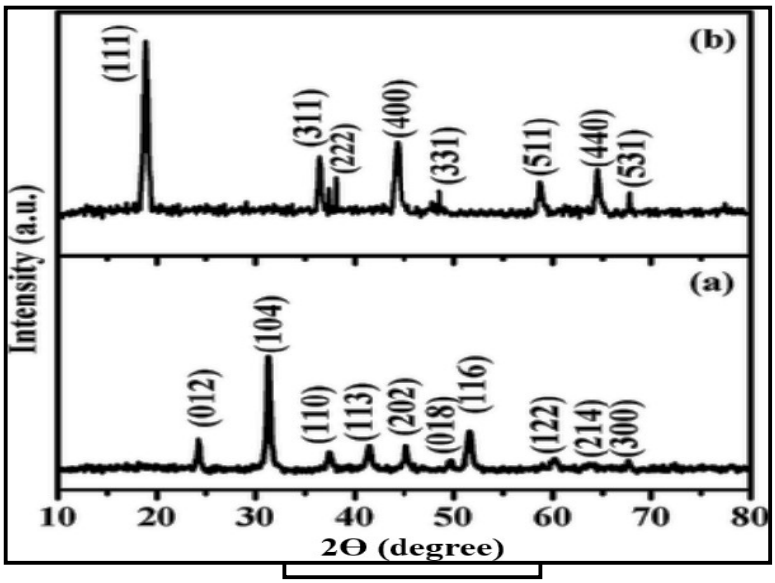

Figure. 3. XRD pattern of (a) as-synthesized precursor (Ni0.25Mn0.75)CO3 microcubes and (b) synthesized porous LNMO microcubes

3.3. MORPHOLOGICAL ANALYSIS

Transmission electron microscopy (TEM) and field emission scanning electron microscopy (FE-SEM) were employed to examine the morphology of the fabricated porous LiNi0.5Mn1.5O4 microcubes (TEM). The synthesised LNMO has a porous microcubes morphology, which is clearly supported by the FE-SEM results, as can be seen in Figure 6.4a, b, which are low and high magnifications of LNMO FE-SEM images of porous LiNi0.5Mn1.5O4 microcubes. The LiNi0.5Mn1.5O4 product is formed of uniform, homogeneously scattered microcubes with an average size of

The porous LNMO microcubes' surface area was calculated using Brunauer-Emmett-Teller measurement (Figure 6.5a), and the precise surface area was found to be 36 m2 g1. The surface area of the porous LNMO microcubes was measured using a N2 adsorption/desorption isotherm study. The LNMO microcubes' pores, which have an aggregated nanopore size of 1.38 nm and a pore volume of 3.62 cm3 g1, are shown in Figure 6.5b. Additionally, the microcubes are evenly spaced apart from one another between adjacent porous microcubes. As a consequence, batteries and supercapacitors perform better electrochemically. This enables effective electron and ion transport.

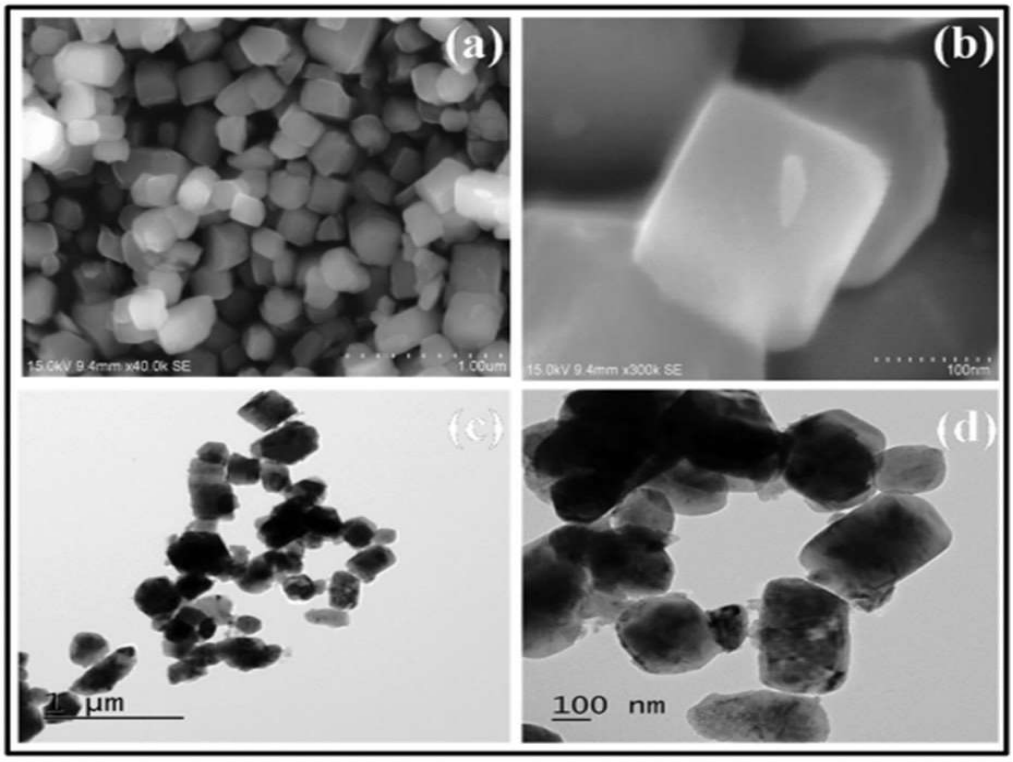

Figure. 4 (a, b) FE-SEM images of porous LNMO microcubes at different magnifications and (c, d) TEM images of porous LNMO microcubes at different magnifications

3.4. BET ANALYSIS

The N2 adsorption/desorption isotherm analysis was used to quantify the surface area of the porous LNMO microcubes using the Brunauer-Emmett-Teller technique. The measurement resulted in a determination of 36 m2 g1 specific surface area. The LNMO microcubes' pores, which have an aggregated nanopore size of 1.38 nm and a pore volume of 3.62 cm3 g1, are shown in Figure 6.5b. Furthermore, the spacing between neighbouring porous microcubes is uniform, allowing for efficient electron and ion transport and, therefore, higher electrochemical performance in batteries and supercapacitors..

3.5. ELECTROCHEMICAL PERFORMANCE IN LI-ION BATTERY APPLICATIONS CV STUDIES

Producing CR2032 coin cells and conducting cyclic voltammetry and charge-discharge analysis on the LNMO cathodes in half-cell lithium-ion batteries were done in order to test the electrochemical performance of the synthesised porous LNMO microcubes. These tests were carried out in order to evaluate the LNMO cathodes. The CV curve of LNMO microcubes measured at a scan rate of 0.1 mV s1 throughout the potential range of 3.5-5.0 V. The presence of Mn4+/Mn3+ may be deduced from the enormous peaks that are seen in the high voltage range, as well as the low intensity peaks that are observed in the area ranging from 3.8 to 4.05 V. The total capacity and total energy of the Ni2+/Ni3+ and Ni3+/Ni4+ redox couples are responsible for the much lower integrated area of the 4 V peaks as compared to the integrated area of the 4.7 V peaks. The plateau that is shown here is evidence of the random dispersion of the Ni and Mn ions that are included inside the crystal structure, as well as the membership of the LNMO microcube particles in the Fd-3m space group [28]. The findings from the XRD experiment, which validated the Fd-3m, is directly connected to the disorder behaviour of the LNMO crystal structure.

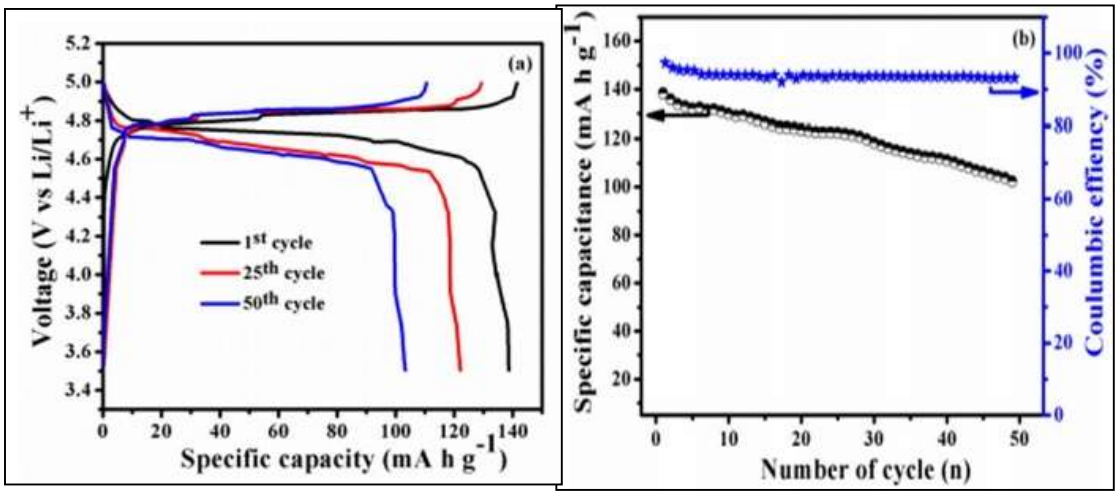

Figure. 5- Cyclic voltammogram of the porous LNMO microcubes in the voltage range of 3.5–5.0 V at a scan rate of 0.1 mV s^{-1}

3.6. CHARGE /DISCHARGE PERFORMANCE

CR2032 coin cells were created in order to test the electrochemical performance of the synthesised porous LNMO microcubes. Utilizing cyclic voltammetry and charge-discharge measurement, the electrochemical performance of the LNMO cathodes in half-cell lithium-ion batteries was also examined. At a scan rate of 0.1 mV s1, Figure 6 shows the CV curve of LNMO microcubes throughout the potential range of 3.5-5.0 V. Because the large peaks show in the high voltage range and the low intensity peaks appear in the range of 3.8 to 4.05 V, it is possible to infer the presence of Mn4+ and Mn3+. The entire capacity and total energy of the Ni2+/Ni3+ and Ni3+/Ni4+ redox couples may be attributed to the peaks at 4.7 V since they have a substantially greater integrated area. The integrated area of the peaks at 4

V is much less than those at 4.7 V. This plateau verifies the earlier explanation [28] that the LNMO microcube particles belong to the Fd-3m space group and that the Ni and Mn ions are distributed ad hoc throughout the crystal structure. The Fd-3m findings from the XRD, which were utilised to validate the Fd, are closely connected to the LNMO crystal structure's disorder behaviour.

3.7. ELECTROCHEMICAL IMPEDANCE SPECTROSCOPY ANALYSIS

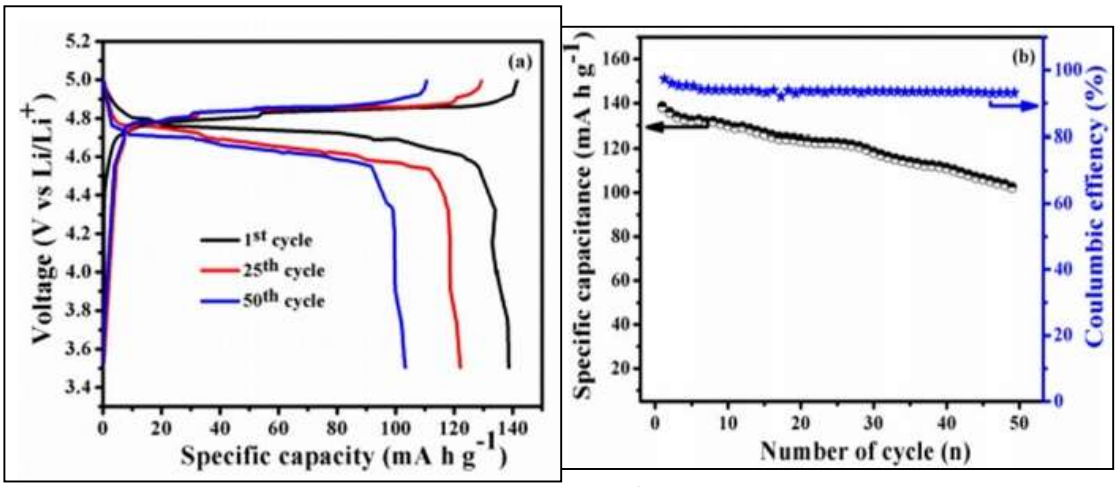

FIGURE. 6 (A) CHARGE–DISCHARGE CURVES 1ST, 25TH AND 50TH CYCLE OF POROUS LNMO MICROCUBES AT 1 C IN THE POTENTIAL RANGE OF 3.5–5.0 V AND (B) SPECIFIC CAPACITY–COULOMBIC EFFICIENCY OF THE OF THE POROUS LNMO MICROCUBES

3.8. ELECTROCHEMICAL IMPEDANCE SPECTROSCOPY ANALYSIS

We further studied the electrochemical kinetics of the LNMO microcubes using electrochemical impedance spectroscopy (EIS) measurements in the frequency range of 10 Hz to 100 KHz. Figure 7 depicts the obtained Nyquist curve for the LNMO cathode materials and displays the curve at the first and fiftyth cycles. In order to determine the precise resistance given by various sources, Z view software was used to create an analogous circuit by fitting EIS measurement data. In order to create an analogous circuit, this was done. Initially, the LNMO microcubes had a low charge transfer resistance (Rct=142), but by the 50th cycle, the homogenous distribution of Ni2+/Ni3+ inside the porous LNMO microcubes prevented the development of a passive layer on the electrode surface, increasing the Rct value to 180. Due to the homogenous distribution of Ni2+/Ni3+ in the porous LN, this transformation took place. This passive layer does not participate in the process by which the electrode dissolves in the electrolyte, preventing the electrode from dissolving and adding to the electrode's high degree of stability. LNMO's porous features make it simpler for additional electrolytes to diffuse to its inner surface, speeding up the electrochemical kinetics reaction. Cathode materials composed of porous LNMO microcubes showed higher discharge plateaus and a higher energy density. However, because to the higher charge potentials, the cyclic performances of porous LNMO

microcubes are now worse than those of LiMn2O4; as a consequence, changing the electrolytes is also crucial for the ongoing research on lithium ion batteries.

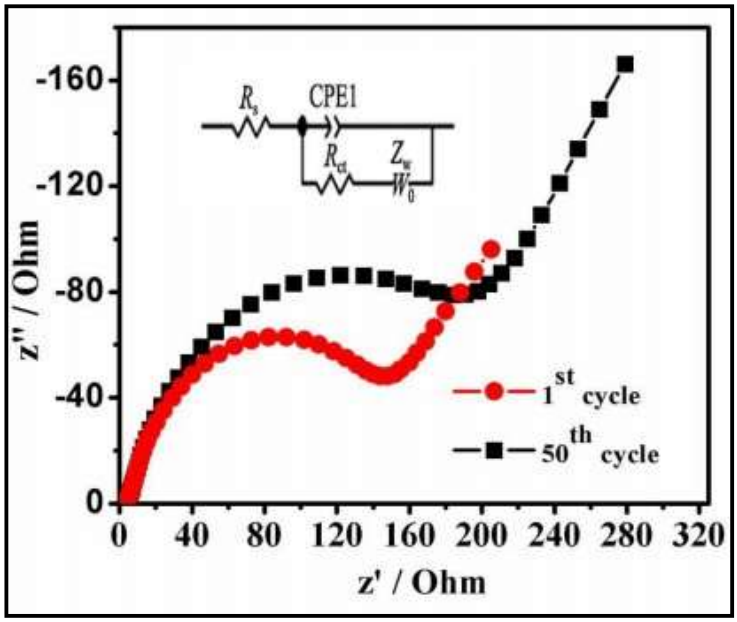

Figure. 7 Electrochemical impedance spectroscopy 1st and 50th cycle of the porous LNMO microcubes

TABLE. 1

COMPRESSION OF PREVIOUSLY REPORTED SPECIFIC CAPACITANCE FOR THE LITHIUMMETAL COMPOUNDS

S.No.	Electrode	Method	Electrolyte	Specific Capacity	Ref.
1	LiAlxMn2−xO4	Conventional solid-state	2 M (NH4)2SO4	160 F g^{-1}	**[37]**
2	LiMn2O4	Microwave-hydrothermal	1 M LiNO3	271 F g^{-1}	**[38]**
3	LiMn2O4	Solid-state	5 M LiNO3	105 mA h g^{-1}	**[39]**
4	Nanoporous LiMn2O	Hydrothermal method	0.5 M Li2SO4	189 F g^{-1}	**[40]**
5	Porous LiNi 0.5Mn1.5O4 microcubes	Precipitation	3 M KOH	294 F g^{-1}	**This work**

The K+ ions have more time to intercalate into and on the surfaces of the active electrode materials when the specific current is lower, which causes a larger specific capacitance than when the specific current is greater. The specific capacitance will, however, drop if the applied current is increased since there won't be enough contact time for cation intercalation. At a current density of 0.75 A g1, the porous LNMO microcubes electrode showed a capacity retention of 97% after 1000 cycles and a maximum specific capacitance of 294 F g1. Table 1 shows the values that have previously been published for lithium metal complexes. When compared to those numbers, the capacitance that was found is quite high. The cathodic process of pseudo capacitance electrochemical behaviour of adsorption/desorption at the electrode/electrolyte interface resulted in a reduction in capacitance in the potential range of 0.6 to 0.4 V during the first discharge cycle. As a result, the electrode/electrolyte contact displayed electrochemical behaviour of adsorption and desorption. The unique porous design and smaller microcubes (163 nm) provide a larger surface area (36 m2 g1), which eventually leads to a stronger reaction current and a quicker electron transfer.

4. CONCLUSIONS

An electrochemical capacitor is made up of two electrodes, an electrolyte, and a separator in the form of an ion-permeable membrane. The great majority of the time, materials that have a thin coating on a current collector are employed to serve as an electrode. In order to achieve the most performance out of the device, it is essential to choose an electrode for a supercapacitor that has a high electrical conductivity, excellent thermal stability, and a large surface area. An electrolyte is ionically conductive due to the fact that it dissolves substances that may separate into ions. In summary, we effectively produced homogeneously dispersed, highly crystalline, and porous LNMO microcubes using a straightforward precipitation process. As a structure-directing agent that promotes the formation of LNMO microcubes, carbonate and sulphate both contribute significantly to changing the morphology of LiNi0.5Mn1.5O4. These two components working together do this. XRD analyses have been used to confirm the LNMO structure's Fd-3m space group. The porous LNMO microcubes had an average size of 163 nm, as seen by the images produced by the FE-SEM and TEM tools. The specific surface area (36.42 m2 g1), pore volume (3.62 cm2 g1), and pore size (1.0 nm), as determined by the BET research, were all excellent (1.41 nm). Batteries have a high discharge capacity even after the first cycle (138.4 mA h g1), and after 50 cycles at 1 C, they have a columbic efficiency of around 93% and a capacity retention of about 74%. The excellent electrochemical performance of LNMO may be attributed to its porous structure, which increases the area of contact between the electrode and the electrolyte and makes the material more permeable to the passage of lithium ions. High electrode stability may also guarantee that Li-ion intercalation and de-intercalation are reversible, which is crucial for the battery's long-term cycle stability. Furthermore, the porous LNMO sub-microcubes' supercapacitive behaviour exhibits a high specific capacity of 294 F g1 at 0.75 A g1 and an outstanding coulombic efficiency of 97% even after 1000 cycles of operation. This research shows that the novel porous microcubes morphological LNMO electrode materials are a competitor as cathode materials for Li-ion batteries and supercapacitors, which may be used in the future for portable electronic devices with improved composition and electrolyte. Future portable

electrical devices with improved composition and electrolyte might employ these materials. Due to its special qualities, such as a high power density, rapid charge/discharge rates, and a long cycle life, supercapacitors are one of the most actively researched issues. When compared to rechargeable batteries, supercapacitors have a far higher power density. Because of this, supercapacitors are a desirable electrochemical device for usage when a rapid surge in power is required. Supercapacitors can be charged and discharged more quickly than batteries when comparing charge/discharge rates, which is a major benefit. Only a steady rate of charging and discharging can be done with batteries. Additionally, they have a long cycle life, which entails that they may experience millions of cycles without experiencing an irreversible chemical reaction. Electric double-layer capacitance is a term used to describe a technique for energy storage that takes advantage of the electric double-layer effect. The contact of the Helmholtz double layer, which is present between the electrode and the electrolyte, is where this process occurs. The amount of charge that can be held at this contact depends on the nature of the electrode surface, its shape, and the kind of electrolyte present, as well as on the voltage that is being applied. By regulating the surface area and pore size, it is possible to create a storage media with a high capacitance.

5. REFERENCES

[1] Ignatiev, X. Chen, N. Wu, Z. Lu and L. Smith, Dalton Trans. **9226,** 5501(2008).

[2] J. Hassoun, K.-S. Lee, Y.-K. Sun and B. Scrosati, J. Am. Chem. Soc. **133,** 3139 (2011).

[3] S.G. Mohamed, C.J. Chen, C.K. Chen, S.F. Hu and R.S. Liu, ACS Appl. Mater. Interfaces **6,** 22701 (2014).

[4] J. Suganya, M. Ramalakshmi, S. Sasikala and P. Shakkthivel, J. Electroanal. Chem. **58,** 720 (2014).

[5] P. Axmann, G. Gabrielli and M. Wohlfahrt-Mehrens, J. Power Sources **301,** 151 (2016)

[6] R. Sehrawat and A. Sil, J. Mater. Sci. 26, 5175 (2015).

[7] Y. Pei, Q. Chen, C.-Y. Xu, H.-X. Wang, H.-T. Fang, C. Zhou, L. Zhen andG. Cao, J. Mater. Chem. A **4,** 9447 (2016).

[8] K. Wang, W. Ren, J. Yang, R. Tan, Y. Liu and F. Pan, RSC Adv. **6,** 47723(2016).

[9] Y.F.K. Amine, H. Tukamoto and H. Yasuda, J. Electrochem. Soc. **143,** 1607(1996).

[10] Q. Zhong, A. Bonakclarpour, M. Zhang and J.R. Dahn, J. Electrochem. Soc. **144,** 205 (1997).

[11] J. Hassoun, S. Panero, P. Reale and B. Scrosati, Adv. Mater. **21,** 4807 (2009).

[12] H.G. Jung, M.W. Jang, J. Hassoun, Y.K. Sun and B. Scrosati, Nat. Commun. **2,** 516 (2011).

[13] J. Xiao, X. Chen, P.V. Sushko, M.L. Sushko, L. Kovarik, J. Feng, Z. Deng, J. Zheng, G.L. Graff, Z. Nie, D. Choi, J. Liu, J.G. Zhang and M.S. Whittingham, Adv. Mater. **24,** 2109 (2012).

[14] S. Li, G. Ma, B. Guo, Z. Yang, X. Fan, Z. Chen and W. Zhang, Electrochim. Acta **55,** 9352 (2016).

[15] Jiao, L. Wang, Y. Zuo, P. Ni and G. Liang, Solid State Ion. **277,** 50 (2015).

[16] R. Madhuvilakku and S. Piraman, Bioresour. Technol. **150,** 55 (2013).

[17] J.S. Park, A.U. Mane, J.W. Elam and J.R. Croy, Chem. Mater. **27,** 1917(2015).

[18] Habib, G., Sharma, S., Ibrahim, S., Ahmad, I., Qureshi, S., & Ishfaq, M. (2022). Blockchain Technology: Benefits, Challenges, Applications, and Integration of Blockchain Technology with Cloud Computing. Future Internet, 14(11), 341.

[19] Ahmed, I., & Yadav, P. K. (2022). Plant disease detection using machine learning approaches. Expert Systems, e13136.

[20] Ahmed, I., & Yadav, P. K. (2022). An Automated System for Early Identification of Diseases in Plant Through Machine Learning. In Soft Computing: Theories and Applications: Proceedings of SoCTA 2021 (pp. 803-814). Singapore: Springer Nature Singapore.